SECURITY CLASSIFICATION OF THIS PAGE

REPORT DOCUMENTATION PAGE

Form Approved
OMB No. 0704-0188

1a. REPORT SECURITY CLASSIFICATION UNCLASSIFIED	1b. RESTRICTIVE MARKINGS
2a. SECURITY CLASSIFICATION AUTHORITY	3. DISTRIBUTION / AVAILABILITY OF REPORT Approved for public release; distribution unlimited.
2b. DECLASSIFICATION / DOWNGRADING SCHEDULE	
4. PERFORMING ORGANIZATION REPORT NUMBER(S) NRL Memorandum Report 6099	5. MONITORING ORGANIZATION REPORT NUMBER(S)
6a. NAME OF PERFORMING ORGANIZATION Naval Research Laboratory 6b. OFFICE SYMBOL (*If applicable*) Code 8320	7a. NAME OF MONITORING ORGANIZATION
6c. ADDRESS (*City, State, and ZIP Code*) Washington, DC 20375-5000	7b. ADDRESS (*City, State, and ZIP Code*)
8a. NAME OF FUNDING / SPONSORING ORGANIZATION SPAWAR 8b. OFFICE SYMBOL (*If applicable*) PMW-142-2	9. PROCUREMENT INSTRUMENT IDENTIFICATION NUMBER
8c. ADDRESS (*City, State, and ZIP Code*) Washington, DC 20363-5100	10. SOURCE OF FUNDING NUMBERS PROGRAM ELEMENT NO.: 64777N; PROJECT NO.:; TASK NO.:; WORK UNIT ACCESSION NO.: DN020-183

11. TITLE (*Include Security Classification*)
Ferromagnetic Mitigation of Electromagnetic Pulse Effects

12. PERSONAL AUTHOR(S)
Maisch, W.G., Vittoria,* C. and Folen, V.J.

13a. TYPE OF REPORT	13b. TIME COVERED	14. DATE OF REPORT (*Year, Month, Day*)	15. PAGE COUNT
Memorandum	FROM 1/86 TO 1/87	1987 October 8	25

16. SUPPLEMENTARY NOTATION
*Present address Northeastern University, Boston, MA

17. COSATI CODES			18. SUBJECT TERMS (*Continue on reverse if necessary and identify by block number*)
FIELD	GROUP	SUB-GROUP	EMP Shielding Ferromagnet

19. ABSTRACT (*Continue on reverse if necessary and identify by block number*)

A realistic description of EMP shielding by ferromagnetic materials was developed in this paper. The attenuation of three pulses by a typical ferromagnetic shield is described. Moreover, the form of this description readily allows for the inclusion of specific properties of ferromagnetic materials (e.g., magnetic relaxation, domain structure and magnetostriction) in calculations of shielding effectiveness.

20. DISTRIBUTION / AVAILABILITY OF ABSTRACT	21. ABSTRACT SECURITY CLASSIFICATION	
☐ UNCLASSIFIED/UNLIMITED ☐ SAME AS RPT ☐ DTIC USERS	UNCLASSIFIED	
22a. NAME OF RESPONSIBLE INDIVIDUAL Vincent J. Folen	22b. TELEPHONE (*Include Area Code*) (202) 767-2595	22c. OFFICE SYMBOL Code 8320.1

DD Form 1473, JUN 86 *Previous editions are obsolete.* SECURITY CLASSIFICATION OF THIS PAGE

Naval Research Laboratory
Washington, DC 20375-5000

NRL Memorandum Report 6099

Ferromagnetic Mitigation of Electromagnetic Pulse Effects

W. G. MAISCH

Radiation Survivability Branch
Condensed Matter and Radiation Sciences Division

C. VITTORIA

Metal Physics Branch
Condensed Matter and Radiation Sciences Division

V. J. FOLEN

Space Applications Branch
Space Systems and Technology Division

October 8, 1987

CONTENTS

FERROMAGNETIC MITIGATION OF ELECTROMAGNETIC PULSE EFFECTS

I. BACKGROUND AND MOTIVATION

Electronic equipment in regions up to 2000 miles in diameter can be made inoperative by electromagnetic pulses (EMP) generated during nuclear detonation. The EMP-induced transients produce electromagnetic fields having electric field magnitudes up to 50 kilovolts per meter. Such fields can produce permanent damage or malfunction, particularly to solid state devices. As a result, entire communications systems can be wiped out by a single nuclear burst. Moreover, EMP can produce currents as large as thousands of amperes in space and ground based electronics systems. Such currents, if not attenuated properly, can destroy any semiconductor device.

There are a number of techniques which can be employed for EMP mitigation. These include the use of extension shields, semiconductors (e.g., zener diodes), spark gaps, thermal and electromechanical devices and filters. Unfortunately, none of the presently used devices are adequate for systems requiring fast rise times and simultaneous large power handling capability.

Ferromagnetic shields may provide a solution to the EMP problem. They can be designed to reflect part of the energy and absorb the rest. Parameters associated with these mechanisms are adjustable within very broad ranges by selecting off-the-shelf materials and appropriate device configurations. Moreover, magnetic media specifically tailored for optimizing EMP mitigation should provide even further improvements. These improvements can be accomplished by tailoring parameters such as magnetic permeability, domain switching time, magnetic relaxation, saturation magnetization and electrical conductivity. New

Manuscript approved July 24, 1987.

materials like metglass (an amorphous ferromagnetic material) can be employed as a substitute to those used previously.

Earlier work has shown [1] that one can obtain a 42 db enhancement of the EMP shielding factor in off-the-shelf ferromagnetic conductors over that in nonferromagnetic conductors. Alternately, the use of ferromagnetic shielding can reduce the weight by an order of magnitude over that required for nonferromagnetic conductors having the same EMP shielding factor. Although this earlier work clearly demonstrates the utility of ferromagnetic shields devised from off-the-shelf materials, a realistic understanding of the behavior of such shields is indeed lacking. This deficiency is principally due to the nonlinear nature of the problem which led earlier workers [1-5] to analytic solutions which oversimplify the magnetization processes involved. Such oversimplifications include models which assume constant or a limiting value of the magnetic permeability. In contrast, realistic descriptions which incorporate actual material characteristics may be obtained with the use of computer solutions. The present report describes such a computer solution. In our approach, we have developed a theoretical model which allows for the inclusion of magnetic relaxation as well as other physical parameters.

II. THEORETICAL FORMALISM

Assume an electromagnetic pulse (Fig. 1) incident on a thin magnetic film with the geometry of Fig. 2.

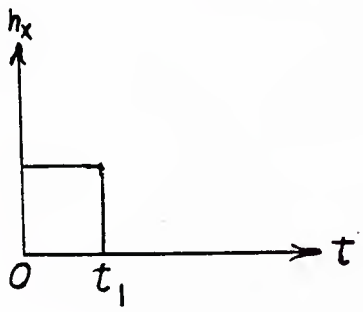

Fig. 1

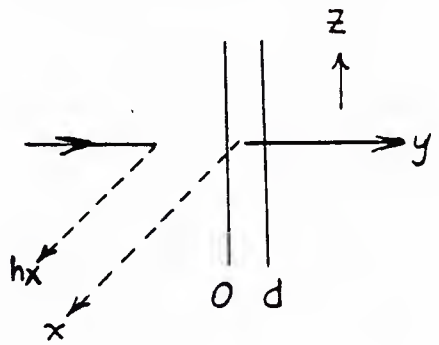

Fig. 2

We then have from Maxwell's equations

$$\nabla \times \vec{e} = -\mu \frac{d\vec{h}}{dt} \tag{1}$$

and

$$\nabla \times \vec{h} = \sigma \vec{e} \quad , \tag{2}$$

where μ and σ are the permeability and conductivity, respectively, of the magnetic film. At this time we also assume that μ is time independent. Using the geometry of Fig. 2 we get

$$\frac{\partial e_z}{\partial y} = -\mu \frac{\partial h_x}{\partial t} \tag{1a}$$

and

$$\frac{\partial h_x}{\partial y} = -\sigma e_z \quad . \tag{2a}$$

Finally, from Eqs. 1a and 2a, we find

$$\frac{\partial^2 h_x}{\partial y^2} = -\sigma \frac{\partial e_z}{\partial y} = \sigma\mu \frac{\partial h_x}{\partial t} \equiv a^2 \frac{\partial h_x}{\partial t} \quad . \tag{3}$$

Taking the Laplace Transform of Eq. 3, we get

$$\frac{\partial^2 h_x(s)}{\partial y^2} = a^2 s\, h_x(s) \quad , \tag{4}$$

whose solution is of the form

$$h_x(s) = A(s)\, e^{-a\sqrt{s}\, y} + B(s) e^{a\sqrt{s}\, y} \quad . \tag{5}$$

To solve for A and B, we introduce the boundary conditions for the electric and magnetic fields at y = 0 and y = d.

$$h_i(t) + h_r(t) = h_x \Big|_{y=0} \quad , \tag{6a}$$

$$z_0 \left[h_i(t) - h_r(t) \right] = - \frac{1}{\sigma} \left. \frac{\partial h_x}{\partial y} \right|_{y = 0} \quad , \tag{6b}$$

$$h_t(t - \frac{d}{c}) = h_x \quad y = d \quad , \tag{6c}$$

and

$$z_0 \, h_t(t - \frac{d}{c}) = - \frac{1}{\sigma} \left. \frac{\partial h_x}{\partial y} \right|_{y = d} \quad , \tag{6d}$$

where z_0 is the free space characteristic impedance. By simple algebraic "manipulations" we obtain

$$h_i(s) = \frac{1}{2} \left[h_x(s) - \frac{1}{z_0 \sigma} \frac{\partial h_x(s)}{\partial y} \right]_{y = 0} \tag{7a}$$

and

$$\left[h_x(s) + \frac{1}{z_0 \sigma} \frac{\partial h_x(s)}{\partial y} \right]_{y = d} = 0 \tag{7b}$$

Substituting Eq. (5) into Eqs. (7a) and 7b) we get

$$h_x(s) = h_i(s) \left[\frac{a_{22}(s) \, e^{-a \sqrt{s} \, y}}{\Delta(s)} - \frac{a_{21}(s) \, e^{a \sqrt{s} \, y}}{\Delta(s)} \right] \tag{8}$$
$$\equiv h_i(s) \, f(s) \quad .$$

This relationship is very much analogous to a relationship found in circuit analysis. We define f(s) as the transfer function of the magneto-conductive medium. We define

$$a_{11}(s) = \frac{1}{2} \left(1 + \frac{a \sqrt{s}}{z_0 \sigma} \right) ,$$

$$a_{12}(s) = \frac{1}{2} \left(1 - \frac{a \sqrt{s}}{z_0 \sigma} \right) ,$$

$$a_{21}(s) = e^{-a \sqrt{s} \, d} \left(1 - \frac{a \sqrt{s}}{z_0 \sigma} \right) \quad ,$$

$$a_{22}(s) = e^{a \sqrt{s} \, d} \left(1 - \frac{a \sqrt{s}}{z_0 \sigma} \right) \quad ,$$

and

$$\Delta(s) = a_{11}(s) \, a_{22}(s) - a_{12}(s) \, a_{21}(s) \quad .$$

We now wish to put f(s) into a form which can be transformed back into the time domain. Substituting the above definitions into Eq. 8 we obtain, after some manipulations

$$f(s) = 2 \sum_{n=0}^{\infty} \frac{(1 - c_1\sqrt{s})^{2n}}{(1 + c_1\sqrt{s})^{2n+1}} e^{-\sqrt{s}} (2nc_2 + ay)$$

$$- \sum_{n=0}^{\infty} \frac{(1 - c_1\sqrt{s})^{2n+1}}{(1 + c_1\sqrt{s})^{2n+2}} e^{\sqrt{s}} (ay - 2c_2 - 2nc_2) \qquad (9)$$

$$\equiv f_1(s) - f_2(s) \quad ,$$

where the summation comes from the expansion of the factor

$$1 - \frac{(1 - c_1\sqrt{s})^2}{(1 + c_1\sqrt{s})^2} e^{-2c_2 s} \quad ,$$

which appears in the denominator of an earlier stage. Here we have let

$$c_1 = \frac{a}{z_0 \sigma}$$

and

$$c_2 = ad \quad .$$

Finally, by expanding all the factors containing $\sqrt{s}$, we get

$$f_1(s) = 2 \left[\sum_{n=0}^{\infty} \sum_{m=0}^{2n} \sum_{p=0}^{\infty} \frac{(-1)^{m+p} c_1^{p+m} (2n+p)!}{(2n-m)!\, m!\, p!} s^{(p+m)/2} e^{-\sqrt{s}(2nc_2+ay)} \right] \qquad (10a)$$

and

$$f_2(s) = 2 \left[\sum_{n=0}^{\infty} \sum_{m=0}^{2n+1} \sum_{p=0}^{\infty} \frac{(-1)^{m+p} c_1^{p+m} (2n+1+p)!}{(2n+1-m)!\, m!\, p!} s^{(p+m)/2} e^{-\sqrt{s}(2c_2+2nc_2-ay)} \right] . \qquad (10b)$$

From reference [6], Table 29.3.87, we have for the Laplace transform

$$s^{\frac{n-1}{2}} \quad e^{-k\sqrt{s}} \qquad \frac{e^{-\frac{k^2}{4t}}}{2^n \sqrt{\pi t^{n+1}}} \quad H_n\left(\frac{k}{2\sqrt{t}}\right)$$

where H_n is the n^{th} order Hermite Polynominal. Therefore, for the transform of f(s), we have

$$f_1(t)=2\left[\sum_{n=0}^{\infty}\sum_{m-0}^{2n}\sum_{p=0}^{\infty} M_1 \frac{e^{-\frac{(2nc_2+ay)^2}{4t}}}{2^{p+m+1}\sqrt{\pi t^{(p+m+2)}}} H_{p+m+1}\left(\frac{2nc_2+ay}{2\sqrt{t}}\right)\right] \tag{11a}$$

and

$$f_2(t)=2\left[\sum_{n=0}^{\infty}\sum_{m-0}^{2n+1}\sum_{p=0}^{\infty} M_2 \frac{e^{-\frac{(2c_2+2nc_2-ay)^2}{4t}}}{2^{p+m+1}\sqrt{\pi t^{(p+m+2)}}} H_{p+m+1}\left(\frac{2c_2+2nc_2-ay}{2\sqrt{t}}\right)\right] \tag{11b}$$

where M_1 and M_2 are the numerical coefficients in Eqs. (10a) and (10b), respectively.

Also, we define

$$f(t) = f_1(t) - f_2(t) \ .$$

Now, we have to convolute the transfer function, f(t with the incident pulse to obtain the transmitted pulse, i.e.,

$$h(t) = \int_0^t f(t-\tau)\ h(\tau)d\tau \tag{12}$$

This completes the derivation.

III. RESULTS AND DISCUSSION

The convolution integral developed in the last section (Eq. 12) has been evaluated for three input pulses (a), a rectangular pulse, (b) a triangular pulse, and (c), a double exponential EMP pulse [7]. Each of these cases will be discussed in detail below following a description of the computer program used to evaluate the convolution integral.

A listing of the computer code is found in the Appendix. It consists of a main program, CONVEMP, and two function subroutines, FLAP and FLAP2. FLAP calculates the transfer function $f(t-\tau)$ and FLAP2 calculates the pulse $h(t)$. There are three versions of FLAP2 listed, one for each of the three pulses mentioned above. In addition to these user subroutines, several library routines are called to evaluate the integral and plot the results. D01AHF is a NAG [8] Library subroutine which integrates the function FLAP2 between the limits TMIN and TB to the relative accuracy EPSR. In our program, FLAP2 calls on FLAP to produce the function FLAP2 = FLAP2 * FLAP, and it is the product function which is integrated. The integral is evaluated repeatedly from t = 0 until some t_{max} when the intensity of the attenuated pulse approaches zero. EZXY and ANOTAT are NCAR [9] Library routines which plot K points of the function FP vs. T and are used in our program to plot the results of the above integrations.

A comment is necessary about the summations which appear in Eqs. 10 and 12. Our program does not contain the sum over l and m explicitly, but includes all terms up to l + m = 1. (Note that the s-dependent part of Eq. 10, the part that undergoes the transform, is dependent only on the sum l + m). Higher terms in the expansion are dependent on higher inverse powers of t and have a small effect near the origin and can be neglected. The sum over n is included explicitly and for most cases there was no significant improvement in increasing n from 10 to 100. However, for certain values of the parameters and at a sufficiently large t there was a small error which could be eliminated by increasing

n to 40. For all the cases discussed below, a value of n = 10 was used. Finally, the high precision (REAL*16) used in FLAP was needed because many of the terms are products of factors containing very large exponentials which exceed the range of lower precision variables.

The last step (before discussing the three pulses) is the evaluation of the constants c_1 and c_2 in terms of the material parameters. We list the appropriate definitions and values below:

$$c_1 = \frac{a}{Z_0 \sigma} \quad ,$$

$$c_2 = ad \quad ,$$

$$a = (\sigma \mu_R \mu_0)^{1/2} \quad ,$$

$$Z_0 = (\mu_0 / \varepsilon_0)^{1/2} \quad ,$$

$$\mu_0 = 4\pi \times 10^{-9} \text{ henry/cm} \quad ,$$

$$\varepsilon_0 = \frac{1}{36\pi} \times 10^{-11} \text{ farad/cm} \quad ,$$

$$\sigma = 5.8 \times 10^{5} \text{ mhos/cm} \quad ,$$

$$d = 1.0 \times 10^{-6} \text{meter} \quad ,$$

$$\mu_R = 500 \quad ,$$

and therefore $c_1 = 0.866366 \times 10^{-8}$

and $c_2 = 1.9090 \times 10^{-4}$.

Furthermore, when y = d, the two factors which appear in the exponentials, $2nc_2 + ay$ and $2nc_2 + 2c_2 - ay$, become equal to $(2n + 1)c_2$. This makes both exponentials the same and greatly simplifies the calculation.

A plot of the transfer function appears in Fig. 3. The curve reaches a maximum of 1.48×10^{4} at $t = 3.2 \times 10^{-9}$sec. and falls to 14.6 at $t = 3.0 \times 10^{-8}$sec.

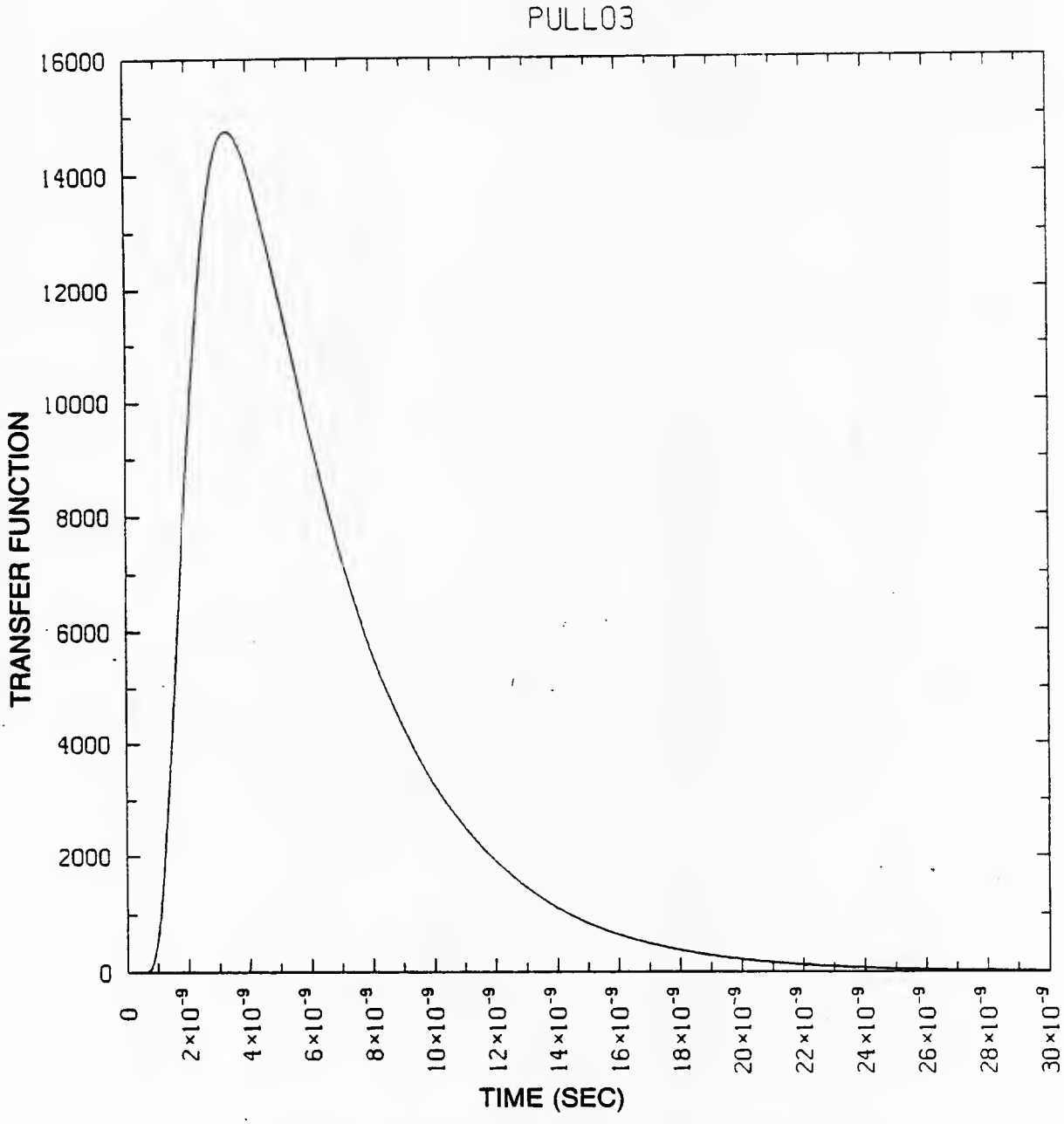

Fig. 3 Plot of Transfer Function vs. Time.

Now let us discuss the three cases. The rectangular and triangular pulses represent simple pulse shapes chosen to check out our program. The EMP pulse (see Eq. 13 below) is one usually used in the literature [7]. The rise time is related to the "unfolding time" of the fission of U^{235} and the decay time is related to the duration of the gamma rays. The widespread use of this curve makes it a suitable choice for the presentation of our calculations.

a) Rectangular Pulse

The incident pulse has the value $h = 1$ for $0 < t < 1.0 \times 10^{-7}$ and $h = 0$ for $t > 1.0 \times 10^{-7}$. Figure 4 shows the attenuated pulse plotted out to $t = 2.0 \times 10^{-7}$. The pulse rises to within one percent of its maximum value of 9.0×10^{-5} at $t = 2.0 \times 10^{-8}$ and falls to 8.0×10^{-7} at $t = 1.2 \times 10^{-7}$.

b) Triangular Pulse

The parameters for the incident pulse are $h = 0$ at $t = 0$, $h = 1.0$ at $t = 1.0 \times 10^{-8}$ and $h = 0$ at $t \geq 1.0 \times 10^{-7}$. Figure 5 shows the attenuated pulse plotted out to $t = 2.0 \times 10^{-7}$. As in the case a) above, the slope of the attenuated curve lags behind that of the incident curve. The pulse rises to a value of 8.25×10^{-5} at $t = 2.0 \times 10^{-8}$ and falls to 3.3×10^{-8} at $t = 1.2 \times 10^{-7}$.

c) EMP Pulse

The incident pulse has the form [7]

$$h = A(e^{-\alpha t} - e^{-\beta t}) \tag{13}$$

with $\alpha = 4.0 \times 10^{6}$ and $\beta = 476.0 \times 10^{6}$ (t in seconds). FLAP2 contains a routine to normalize the peak to unity. The maximum occurs at $t = 1.0 \times 10^{-8}$. Figure 6 shows the attenuated pulse plotted out to $t = 1.0 \times 10^{-6}$. The pulse rises to 8.8×10^{-5} at $t = 2.5 \times 10^{-8}$ and falls to 1.6×10^{-6} at $t = 1.0 \times 10^{-6}$.

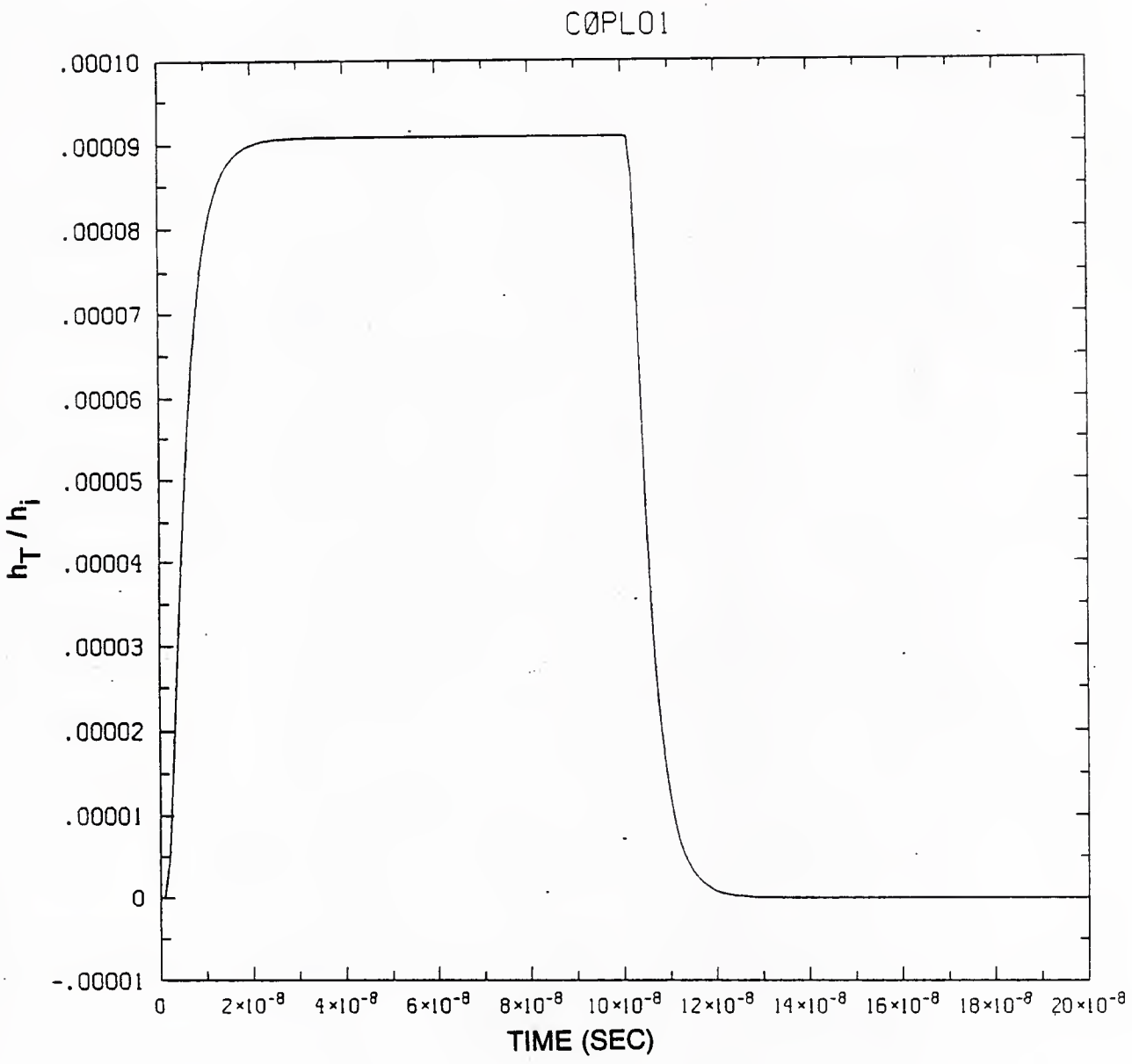

Fig. 4 Plot of h_T/h_i vs. Time for a Rectangular Pulse having an amplitude of 1 for $0 \leq T \leq 1.0 \times 10^{-7}$ sec. and 0 for $T > 1.0 \times 10^{-7}$ sec.

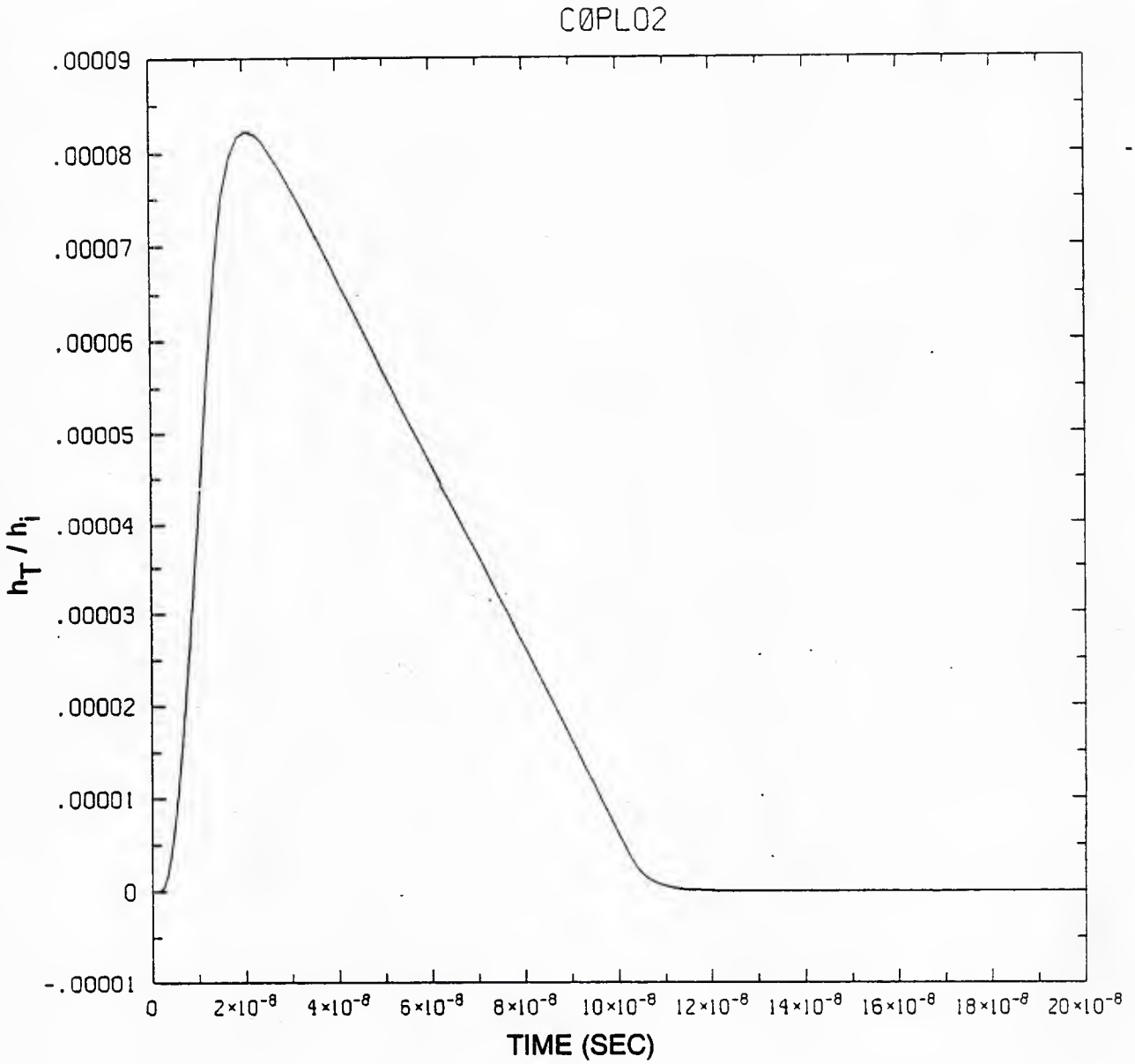

Fig. 5 Plot of h_T/h_i vs. Time for a Triangular Pulse having an amplitude of 1 for T = 1.0 x 10^{-8} sec. and 0 at T = 0 and T $\geq$ 1.0 x 10^{-7} sec.

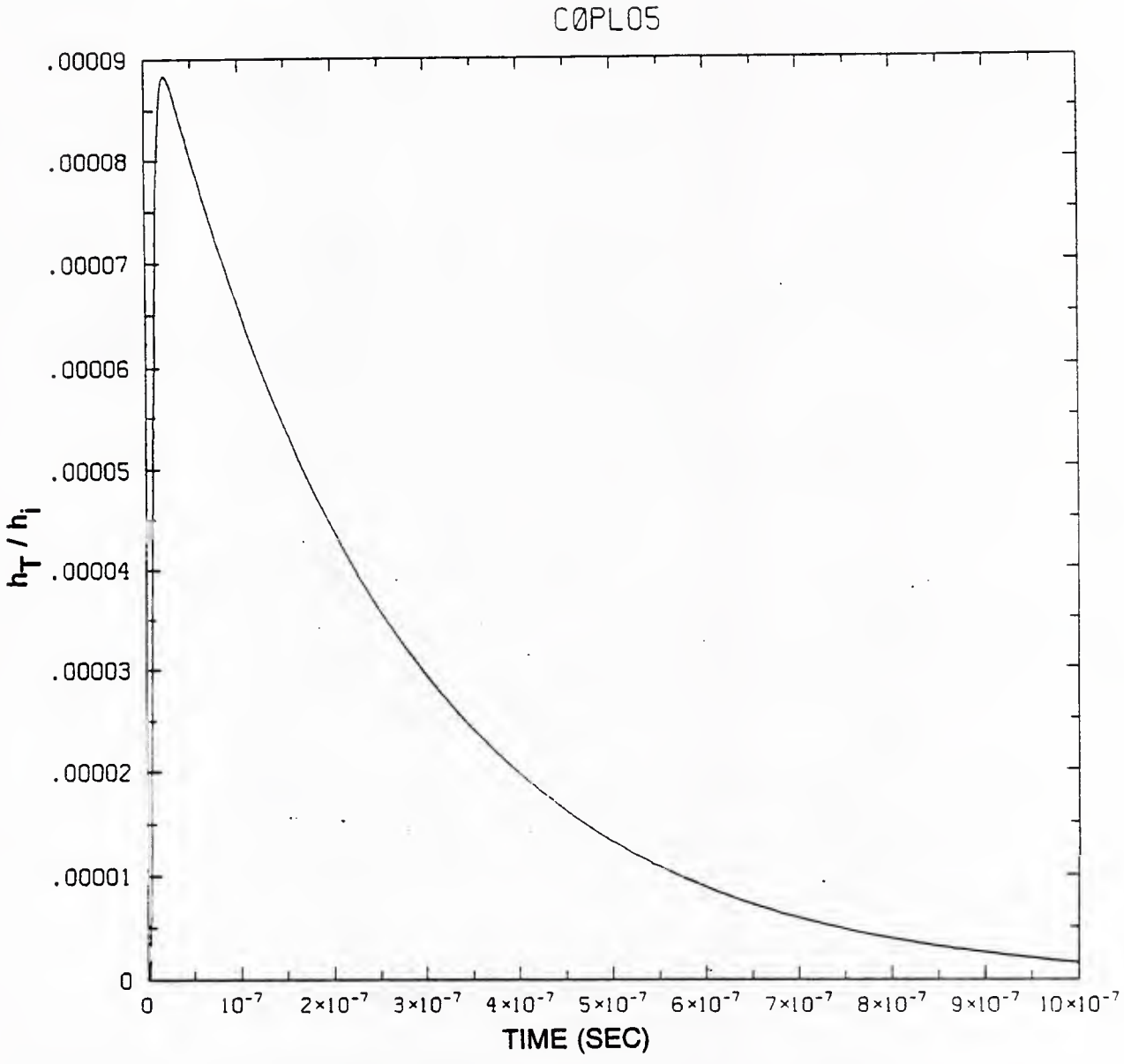

Fig. 6 Plot of h_T/h_i vs. Time for a pulse having the form $h_i = A(e^{-\alpha T} - e^{-\beta T})$ with $\alpha = 4.0 \times 10^6$, $\beta = 476.0 \times 10^6$ and A chosen so that $h_{max} = 1$.

In all of these examples the transmitted pulse is not only attenuated but delayed and distorted. This is most easily seen in the transfer function itself, which shows the transmission of a delta function input pulse. The distortion results from the progressively greater attenuation of higher frequency components in the signal. The large attenuations obtained result primarily from reflection at the front surface, so that even very thin material can be an effective shield against radiation fields. With the method of calculation used, any influence of the back surface on this reflection is included.

As shown here, we have developed a realistic description of EMP shielding by ferromagnetic materials, including the attenuation of three pulses by a typical ferromagnetic shield. Moreover, the form of this description readily allows for the inclusion of specific properties of ferromagnetic materials (e.g., magnetic relaxation, domain structure and magnetostriction) in calculations of shielding effectiveness.

REFERENCES

1. R.R. Ferber and F.J. Young, "Enhancement of EMP Shielding by Ferromagnetic Saturation," IEEE Trans. NS-17, 354, (1969).

2. L.W. Richetts, J.E. Bridges and J. Miletta, EMP Radiation and Protective Techniques," John Wiley & Sons 1976.

3. D.E. Merewether, "Electromagnetic Pulse Transmission through Thin Sheet of Saturable Ferromagnetic Material of Infinite Surface Area," IEEE Trans. on Electromagnetic Compatibility, EMC-11, No. 4, p. 139, Nov. 1969.

4. D.E. Merewether, "Analysis of the Shielding Characteristics of Saturable Ferromagnetic Shields," IEEE Trans. on Electromagnetic Compatibility, EMC-12, No. 3, p. 134, Aug. 1970.

5. W.J Karzas and Tse Chin Mo, "Linear and Nonlinear EMP Diffusion through a Ferromagnetic Conducting Slab," IEEE Trans. on Electromagnetic Compatibility, EMC-20, No. 1, p. 118, Feb. 1978.

6. M. Abramowitz and I. Stegun, editors, Handbook of Mathematical Functions," Dover Publications, New York, NY, 1965.

7. R.N. Ghose, "EMP Environment and Systems Hardness Design," Don White Consultants, Inc., Gainesville, VA, 1984.

8. "EMP Engineering and Design Principles," Bell Telephone Labs, Technical Publication Dept., 1985.

9. W.J. Karzas and R. Latter, Phys. Rev. 126, 1919 (1962).

10. NAG Fortran Library , Numeric Algorithms Group, Downer's Grove, IL.

11. SCD Graphics System, National Center for Atmospheric Research, Boulder, CO.

```
      PROGRAM CONVEMP
      CHARACTER IDENT*8,YN*1,DUM*1
      DIMENSION FP(2001),T(2001),DT(3),XLAB(2),IW(102),TN(10),NPI(10)
      REAL*8 Y,Y0,FLAP2,D01AHF,EPSABS,EPSREL,ABSERR,W(800),TMIN,TI,
     1FL(10),EPSR,RELERR,TB
      REAL*16 PI,PIR2,XM1,F0
      EXTERNAL FLAP2
      COMMON /FBLK/C1,C2,PIR2,ALPHA,F0,NMAX,/FBLK3/TMIN,TI,FL12,
     1NI,NPI,TN,FL,NF
      DATA C1/8.6637E-9/,C2/1.9090E-4/,XLAB/'TIME','$'/,YLAB/'F$'/
      CALL DATE(DT)
      TYPE*,'C1 = ',C1,' C2 = ',C2
5     TYPE*,'RUN IDENTIFICATION (FILENAME)?'
      IDENT='        '
      ACCEPT 135,IDENT
C EXPANSION OF DENOMINATOR
      TYPE*,'HIGHEST VALUE OF N IN SUMMATION?'
      ACCEPT*,NMAX
      TYPE*,' INPUT FOR FLAP2'
      NF=0
C ACCEPT INPUT FROM PULSE SUBROUTINE
      Y0=FLAP2(0.)
      PRINT 100,CHAR(27),CHAR(15)
      PRINT 105,DT
      PRINT 145,IDENT
      PRINT 160,NI
      PRINT 115,NMAX
      NF=-1
C PRINT INPUT FROM PULSE SUBROUTINE
      Y0=FLAP2(0.)
      PRINT 130,CHAR(12),CHAR(18),CHAR(27)
      NP=0
      TYPE*,'SUPPRESS PRINTING (Y/N)?'
      ACCEPT 140,YN
      IF(YN.EQ.'Y') NP=1
      TMAX=TMAX*1.E-6
      IDENT(7:7)='$'
      XM1=-1.
      PI=QACOS(XM1)
      PIR2=SQRT(PI)
      T(1)=0.
      IPT=IMAX+1
      Y=0.
      FP(1)=0.
      EPSR=1.E-5
      TMIN=0.
      NLIMIT=0
      IFAIL=0
      IT1=1
      T00=0.
      IIT=0
```

```
C EVALUATE CONVOLUTION INTEGRAL AT POINT TI IN INTEGRATION REGION I
C NEXT I
      DO 20 I=1,NI
      T0=(TN(I+1)-TN(I))/NPI(I)
      IPT=NPI(I)+1
      IF(I.GT.1) IIT=IIT+NPI(I-1)
C NEXT TI
      DO 20 IT=2,IPT
      TI=TN(I)+T0*(IT-1)
      K=IIT+IT
      T(K)=TI
      ALPHA=-C2
      Y=0.
      NCJ=0
C PERFORM INTEGRATION OVER EACH INTEGRATION REGION J UP TO POINT TI
      DO 30 J=1,NI
      NF=J
      IF(NCJ.EQ.1) GO TO 30
      IF(FL(J+1).LT.0.) GO TO 30
      TMIN=TN(J)
      TB=TN(J+1)
      IF(TI.LE.TN(J+1)) THEN
      TB=TI
      NCJ=1
      ENDIF
      TYPE*,T0,TN(I),TI,TB
C NAG INTEGRATION ROUTINE
      Y0= D01AHF(TMIN,TB,EPSR,NPTS,RELERR,FLAP2,NLIMIT,IFAIL)
      Y=Y+Y0
30    CONTINUE
20    FP(K)=Y
C NCAR PLOTTING ROUTINES
      CALL ANOTAT(XLAB,YLAB,1,0,0,%REF(DUM))
      CALL EZXY(T,FP,K,%REF(IDENT))
      IF(NP.EQ.0) THEN
      PRINT 100,CHAR(27),CHAR(15)
      PRINT 120
C PRINT OUTPUT AT SELECTED POINTS ONLY
      DO 10 J=1,K,10
      IF(J.EQ.1)GO TO 10
      IF(MOD((J-1),40).EQ.0) PRINT 125,(T(I),FP(I),I=(J-30),J,10)
10    CONTINUE
      PRINT 130,CHAR(12),CHAR(18),CHAR(27)
      ENDIF
      TYPE*,'ENTER ANOTHER SET OF DATA (Y/N)?'
      ACCEPT 140,YN
      IF(YN.EQ.'Y') GO TO 5
100   FORMAT(1X,A1,'[5i',A1)
105   FORMAT(' DATE = '2A4,A1)
115   FORMAT(' LAST TERM IN EXPANSION, N = ',I5)
120   FORMAT(5X,4(4X,'TIME',10X,'FCONV',7X))
```

```
125   FORMAT(5X,4(E12.4,2X,E14.5,2X))
130   FORMAT(1X,3A1,'[4i')
135   FORMAT(A8)
140   FORMAT(A1)
145   FORMAT(1X,A8)
160   FORMAT(' NO. OF INTEGRATION REGIONS = ',I5)
      STOP
      END
C THIS ROUTINE CALCULATES THE TRANSFER FUNCTION
      REAL*8 FUNCTION FLAP(TAU)
      REAL*16 CK1,X1,EX1,F,F1,F2,F3,F10,F1S,F2S,F3S,PIR2
      REAL*8 TI,FLAP2,TAU,TI0,TMIN
      COMMON /FBLK/C1,C2,PIR2,ALPHA,F,NMAX,/FBLK2/X1,EX1,CK1,F1S,F2S,F3S,
     1/FBLK3/TMIN,TI0
      TI=TI0-TAU
      IF((TI**2).EQ.0..OR.TI.LT.0.) THEN
      FLAP=0.
      RETURN
      ENDIF
      F=0.
      F1S=0.
      F2S=0.
      F3S=0.
      CK1=1./(PIR2*TI**1.5)
      ALPHA=-C2
      DO 10 N=0,NMAX
      ALPHA=ALPHA+2.*C2
      ALPHA2=ALPHA*ALPHA
      X1=ALPHA2/(4.*TI)
      EX1=EXP(-X1)
      F10=C1*CK1*EX1
      F1=-2.*F10
      F2=C2*F10*(C2+6*C1)*(2*N+1)**2/TI
      F3=-C1*C2**3*F10*(2*N+1)**4/TI**2
      F=F+F1+F2+F3
      F1S=F1S+F1
      F2S=F2S+F2
      F3S=F3S+F3
10    CONTINUE
      FLAP=F
      RETURN
      END
```

```
C THIS ROUTINE GENERATES A RECTANGULAR PULSE
      REAL*8 FUNCTION FLAP2(TAU)
      REAL*8 TAU,TB,T,FL(10),TMIN,FLAP
      DIMENSION TN(10),NPI(10)
      COMMON /FBLK3/TMIN,TB,FL12,NI,NPI,TN,FL,NF
      DATA TN(1)/0./,FL(1)/1./
C INPUT PULSE PARAMETERS
      IF(NF.EQ.0) THEN
      TYPE*,'NUMBER OF INTEGRATION REGIONS?'
      ACCEPT*,NI
      TYPE*,'FOR EACH REGION, NUMBER OF POINTS, VALUE OF FUNCTION,
     1AND END POINT?'
      DO 10,I=1,NI
      TYPE*,'REGION NO. ',I
      ACCEPT*,NPI(I),FL(I+1),TN(I+1)
10    TN(I+1)=TN(I+1)*1.E-6
      RETURN
      ENDIF
C PRINT PULSE PARAMETERS
      IF(NF.EQ.-1) THEN
      PRINT 110
      PRINT 115,(NPI(I),TN(I+1),FL(I+1),I=1,NI)
      RETURN
      ENDIF
C CALCULATE PULSE
      FLAP2=FL(2)
      FL12=FLAP2
      FLAP2=FLAP2*FLAP(TAU)
110   FORMAT(2X,'NPTS',4X,'TMAX',9X,'FL')
115   FORMAT(1X,I5,2E12.3)
      RETURN
      END

C THIS ROUTINE GENERATES A TRIANGULAR PULSE
      REAL*8 FUNCTION FLAP2(TAU)
      REAL*8 TAU,TB,T,FL(10),TMIN,FLAP
      DIMENSION TN(10),NPI(10)
      COMMON /FBLK3/TMIN,TB,FL12,NI,NPI,TN,FL,NF
      DATA TN(1)/0./,FL(1)/1./
C INPUT PULSE PARAMETERS
      IF(NF.EQ.0) THEN
      TYPE*,'NUMBER OF INTEGRATION REGIONS?'
      ACCEPT*,NI
      TYPE*,'FOR EACH REGION-NUMBER OF POINTS,VALUE OF FUNCTION,
     1AND END POINT(MICROSECONDS)?'
      DO 5,I=1,NI
      TYPE*,'REGION NO. ',I
      ACCEPT*,NPI(I),FL(I+1),TN(I+1)
5     TN(I+1)=TN(I+1)*1.E-6
      RETURN
      ENDIF
```

```
C PRINT PULSE PARAMETERS
      IF(NF.EQ.-1) THEN
      PRINT 110
      PRINT 115,(NPI(I),TN(I+1),FL(I+1),I=1,NI)
      RETURN
      ENDIF
C CALCULATE PULSE AT POINT TAU IN REGION NF
      GO TO (10,20) NF
10    A1=FL(2)/TN(2)
      FLAP2=A1*TAU
      FL12=FLAP2
      FLAP2=FLAP2*FLAP(TAU)
      RETURN
20    DELT=TN(3)-TN(2)
      A2=-FL(2)/DELT
      B2=FL(2)*TN(3)/DELT
      FLAP2=A2*TAU+B2
      FL12=FLAP2
      FLAP2=FLAP2*FLAP(TAU)
110   FORMAT(2X,'NPTS',4X,'TMAX',9X,'FL')
115   FORMAT(1X,I5,2E12.3)
      RETURN
      END

C THIS ROUTINE GENERATES A DOUBLE EXPONENTIAL EMP PULSE
      REAL*8 FUNCTION FLAP2(TAU)
      REAL*8 TAU,TB,T,FL(10),TMIN,FLAP,GAMMA,GAMMA1,EX,C1,A
      DIMENSION TN(10),NPI(10)
      COMMON /FBLK3/TMIN,TB,FL12,NI,NPI,TN,FL,NF
      DATA TN(1)/0./,TN(2)/1.E-8/,TN(3)/1.E-7/,NI/3/,A0/1./
      SAVE A
C INPUT PULSE PARAMETERS
      IF(NF.EQ.0) THEN
      TYPE*,'NUMBER OF POINTS, END POINT (MICROSECONDS)?'
      ACCEPT*,NPI(4),TN(4)
      TN(4)=TN(4)*1.E-6
      TYPE*,'ALPHA, BETA?'
      ACCEPT*,FL(1),FL(2)
      DO 10,I=1,2
10    FL(I)=FL(I)*1.E6
      NPI(1)=25*NPI(4)/100
      NPI(2)=NPI(1)
      NPI(3)=2*NPI(1)
C NORMALIZE CURVE TO A0
      GAMMA=FL(2)/FL(1)
      GAMMA1=GAMMA-1
      TMAX=LOG(GAMMA)/(FL(1)*GAMMA1)
      EX=1.+1./GAMMA1
      C1=GAMMA1/GAMMA**EX
      A=A0/C1
      RETURN
      ENDIF
```

```
C PRINT PULSE PARAMETERS
      IF(NF.EQ.-1) THEN
      PRINT 105,NPI(4),TN(2)
      PRINT 100,FL(1),FL(2)
      PRINT 110,C1,TMAX
      RETURN
      ENDIF
C CALCULATE PULSE AT POINT TAU
      FLAP2=A*(EXP(-FL(1)*TAU)-EXP(-FL(2)*TAU))
      FL12=FLAP2
      FLAP2=FLAP2*FLAP(TAU)
100   FORMAT(' ALPHA = ',E12.3,' BETA = ',E12.3)
105   FORMAT(' NPTS = ',I5,' T = ',E12.3)
110   FORMAT(' E(MAX)/A = ',F7.5,' TMAX = ',E12.3)
      RETURN
      END
```

DEPARTMENT OF THE NAVY

NAVAL RESEARCH LABORATORY
Washington, D.C. 20375-5000